POAC'17
Busan, KOREA

Proceedings of the 24th International Conference on
Port and Ocean Engineering under Arctic Conditions
June 11-16, 2017, Busan, Korea

A Study of Ice Oblique Drift Action onto the Structure Partially Sheltered by another Object

Marina M. Karulina[1,4], Alexander N. Sakharov[3,4], Aleksey V. Marchenko[2,4],
Evgeny B. Karulin[1,4], Peter V. Chistyakov[3,4]
[1]Krylov State Research Centre, St.-Petersburg, Russia
[2]The University Centre in Svalbard, Longyearbyen, Norway
[3]Moscow State University, Moscow, Russia
[4]Sustainable Arctic Marine and Coastal Technology (SAMCoT), Centre for Research-based Innovations (CRI), Norwegian University of Science and Technology, Trondheim, Norway

ABSTRACT

Ice action on a structure may follow different scenarios primarily depending on ice environment (conditions) and type (shape) of the structure itself. The study examines a case of oblique drift ice acting on a structure partially sheltered by another object (offshore structure) or Ice Protection Structure (IPS). This scenario was investigated in a model experiment whose purpose was to study ice effect on support beams (foundations) placed near each other. The supports had extended side walls and rectangular plan form. The paper contains main results of the model experiment showing that the rear support partly sheltered by the forward support was subject to impulse ice loads. The magnitude of ice load impulse is determined by the splitting force acting on the ice sheet section enclosed between the two units, and such magnitudes can be quite significant. In March 2016 two mesoscale tests were conducted in sea ice of about 0.6 m thickness in a fjord of Svalbard archipelago to study this process. The tests consisted in loading of short ice cantilevers by horizontal force distributed over one of the specimen side. The cantilevers had triangular form in plan. The test procedure and load measurements are described. The ice sheet failure analysis is performed using both a simple engineering approach and an analytical model.

KEY WORDS: Ice loads, Ice failure, Splitting, Tensile stress, Compressive stress

INTRODUCTION

For specification of design ice loads on engineering structures it is required to investigate and analyze all potential ice exposure scenarios and identify the worst cases of ice impact levels. As a rule, the global ice load on a structure is governed by a so-called "limit stress scenario" when ice cover is broken in interaction with the structure. It is assumed that external driving forces acting on the ice cover are sufficient to break it, while the failure modes can be of various types. In accordance with ISO 19906 (2011) the "limit stress scenario" includes ice floe splitting cases when ice may interact with part rather than total width of the structure. Some specific cases of ice cover splitting are addressed in Bhat (1988), Sodhi and Chin (1995) where formulas for estimation of splitting forces are given for the cases under consideration. Ice floe splitting (when part of the ice cover is broken off) can be expected to occur at an "oblique" ice drift at a glance ice impact on a structure which is sheltered by another object. This kind of situations may happen, e.g., in case of ice protection barriers or system of offshore field facilities (Figure 1).

An interesting case of the scenario under consideration is ice interaction with the substructure blocks installed on the Philanovsky field in the northern part of the Caspian Sea. The substructure consists of two extended parallel structures (blocks) of pentagonal planform (Figure 1, right). At some directions of ice drift the rear block is partly sheltered by the front one, and, as shown by earlier published model ice test data (Karulina et al., 2012), the rear support will periodically break off quite large ice floes. In these scenarios the maximum global force on this block will be governed by ice splitting forces.

Ice protection barriers near the drilling structure (Schiff & Hafen, 2008) | Platforms on Philanovsky field, Caspian Sea (www.lukoil.ru)

Figure 1. Examples of the offshore structures arrangement

It the purpose of this study to investigate the ice cover failure mechanism and to estimate ice loads on the structure sheltered by another object. The study is based on some results of model tests in ice basin (Karulina et al., 2012), as well as on the data of special-purpose meso scale tests conducted in sea ice with subsequent analysis of these tests. The tests were carried out under the international project SAMCoT, WP1, and partly reproduced the ice/structure interaction scenario under study here.

INVESTIGATION OF OBLIQUE ICE DRIFT IN ICE BASIN

Ice interactions with the platforms designed for the Philanovsky field were investigated on models at different ice drift directions at the ice basin of Krylov State Research Centre (KSRC), St.Petersburg. As it is seen in Figure 1, right, the substructure consists of two parallel extended blocks. The internal and end side surfaces of these structures are made as vertical walls, while the external sides have inclined flat surfaces in way of interaction with ice. This study examines a scenario when the rear structure is partly sheltered by the front structure and analyzes global ice loads on the rear structure. This model test case is illustrated in Figure 2.

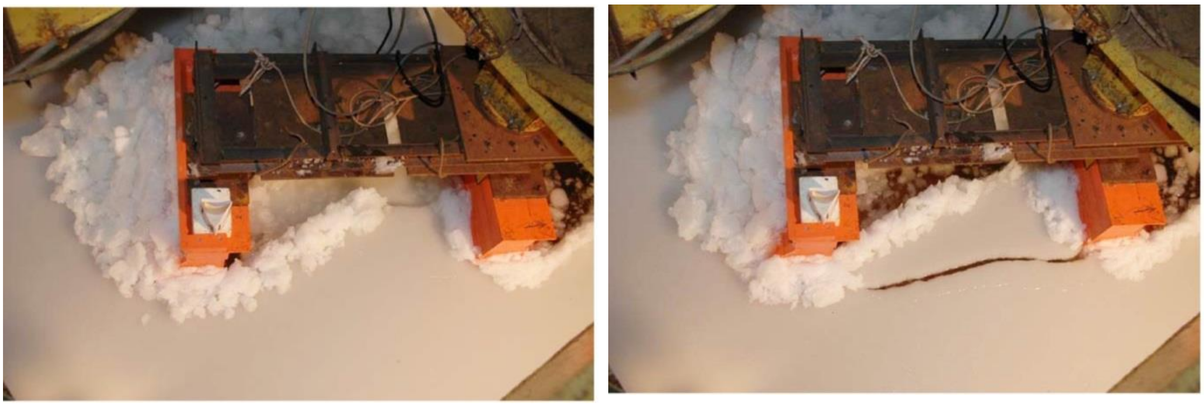

a) Ice crushing on internal and end side of rear block

b) Formation of macrocrack

Figure 2. Ice model tests of platform foundation consisting of two blocks

Figure 3 shows step-wise failure of a level ice field drifting towards the substructure at an angle β:

- –Initially the ice edge comes into contact and interacts with the front structure, then the ice breaks against the vertical end surface and inclined external side surface of the structure (Figure 3a)
- –When the ice edge comes into contact with the rear block it crumbles against its vertical internal and end surfaces (Figure 3b). This process can also be observed from a photo taken during the model tests (Figure 2a).
- –The crushed ice area at the internal surface is gradually increasing, which cause the global ice load to grow. Once a certain load is achieved to initiate a macro crack in ice between two blocks, an ice floe is splitted (Figure 3c and 2b). The crack inception occurs at the stress raiser – edge where the end side and internal surface of the block intersect.
- –Drifting ice is pushing the split ice floe between the blocks into a channel behind the facility.

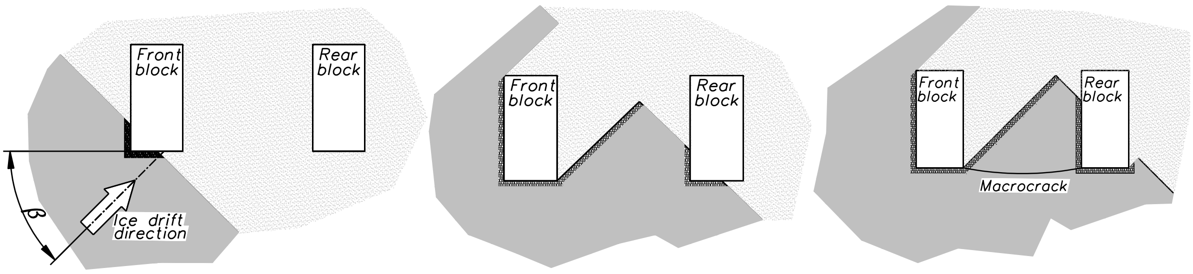

a) Front block interaction with ice

b) Ice cruching against the rear block

c) Formation of macrocrack

Figure 3. The ice action stages

Then the above-described processes are repeated. A cyclic pattern of interaction between the rear block and ice governs the global ice load behaviour. Figure 4 shows variation of the horizontal ice force component acting normally to the internal side surface of the rear structure. The force was recorded in the ice model tests (Karulina et al., 2012) and extrapolated to full-scale condition. The ice drift angle was 45°, ice thickness 1.2 m, drift speed 0.5 m/s. The peak load values at the time of splitting (macro crack inception) are in the range of 10.2 – 12.8 MN (average peak value is 11.4 MN), then the load falls to practically zero values. The average peak load period is 70 s.

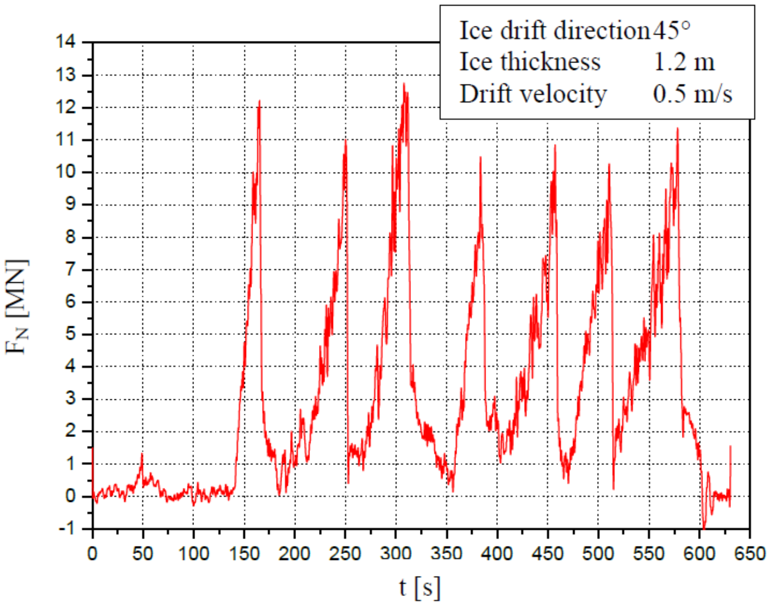

Figure 4. Normal ice force acting on rear block.

Apart from the cyclic pattern of ice action on the rear block, it can be expected that the rear block will be subject to quite a large turning moment about the vertical axis due to asymmetrical application of ice force (with only one peripheral side of the structure interacting with ice). This factor affects the ability of the structure to resist shearing force and should be taken into consideration for design, however in this study it is left out of consideration.

One of the causes for macro cracking and ice floe splitting can be a bending moments generated by the forces F_N and F_T about the point B – crack tip on the front block edge (Figure 5). F_N and F_T are normal and tangential forces acting on the exposed part of ice field from rear block, accordingly. Tensile stresses at the point A – crack base can be approximately estimated based on the theory of cantilever beams using a simple formula of ultimate bending strength $\sigma_f = \frac{6M}{hW^2}$, where M is the total moment of forces F_N and F_T about the point B, h is ice thickness, W is crack length, which is determined by the distance between blocks in this case. If thus obtained value $\sigma_f = 0.412$ MPa exceeds the ice bending strength in horizontal plane, then bending moments acting on the exposed part of ice field may cause cracking.

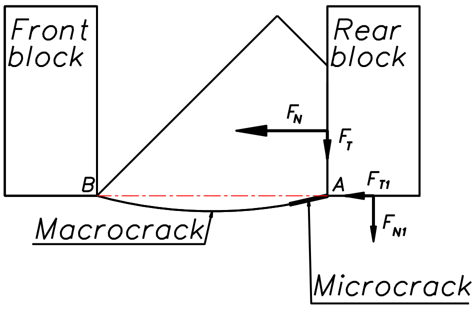

Figure 5. Forces acting from rear block on ice cover.

Another approach to analyzing the causes of ice floe splitting is based on representation of the rear block as a rectangular indenter penetrating ice with its corner edge. The process of radial cracks initiation and propagation at penetration of a structure into ice that cause ice floe splitting is described by Bhat (1988). In the case under consideration the forces acting on ice from the internal (F_N, F_T) and end (F_{N1}, F_{T1}) faces of the rear block contribute to transformation of a micro crack at the corner (point A) into the splitting macro crack (Figure 5).

For further investigation of macro cracking mechanisms mesoscale in-situ tests were performed in full scale ice to reproduce a similar scenario of ice cover loading and breaking. The tests are described in more detail below.

IN-SITU TESTS WITH HORIZONTAL LOADING OF SHORT ICE CONSOLES

Test Set-up and Equipment

In March 2016 two in-situ tests were performed in a fjord of Svalbard archipelago using floating ice specimens of right-angle triangle and rectangular trapezium planforms.

Figures 6 and 7 show the test set-up and dimensions of test specimens. The specimens were cut from ice so that one of their edges remained attached to the ice field. For the purposes of these experiments the length of uncut edge was important rather than the shape of specimens. It was 0.7 m for the triangular specimen and 1.2 m for the trapezium. In the following these are referred to as the “narrow” and the “wide” specimen, respectively.

A horizontal force was applied to one of the free side surfaces using a 600×800 mm vertical plate driven by a rig of two hydraulic cylinders capable to exert a total horizontal force of about 600 kN (Figure 6). The rig is equipped with displacement and pressure gages whose indications were recorded by computer.

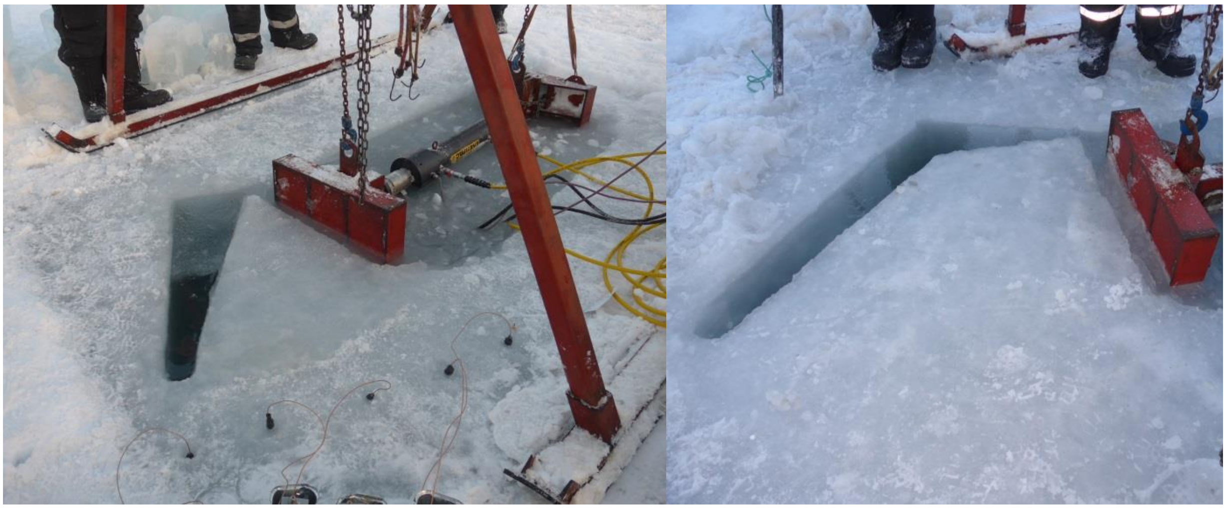

Loading of triangle ("narrow") specimen Loading of trapezium ("wide") specimen

Figure 6. Test set-up.

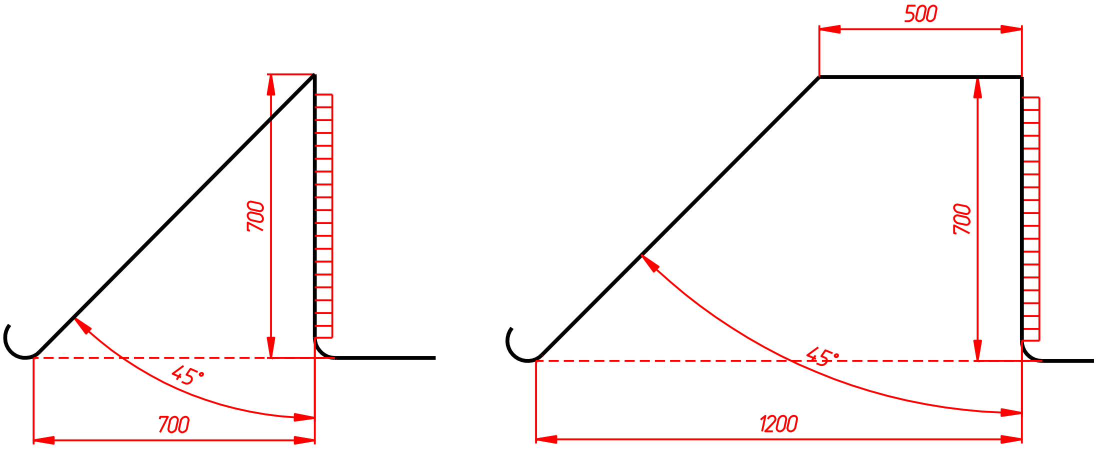

Figure 7. Dimensions of ice specimens

The tests were conducted at ice thickness of 0.6 m, ice temperature –3.5°C and salinity 4.5 ppt averaged over thickness. The horizontal plate speed is 1.5 mm/s. The tests were performed in sea ice and have some characteristic differences from the model tests in ice basin with simulation of ice loads on structures:

– The size and thickness of loaded ice section have the same order of magnitude, while in model experiments the linear dimensions of split ice section were by an order of magnitude greater than its thickness;
– The in-situ test setup prevented normal displacement of the loading plate with respect to the loading force on block, which excluded any friction force shown in Figure 5.

Description of Ice Failure Processes

Failure modes of ice cantilevers were analyzed based on synchronized records of forces (Figure 8) and test videos. Figures 9 and 10 show crack patterns obtained during testing of specimens.

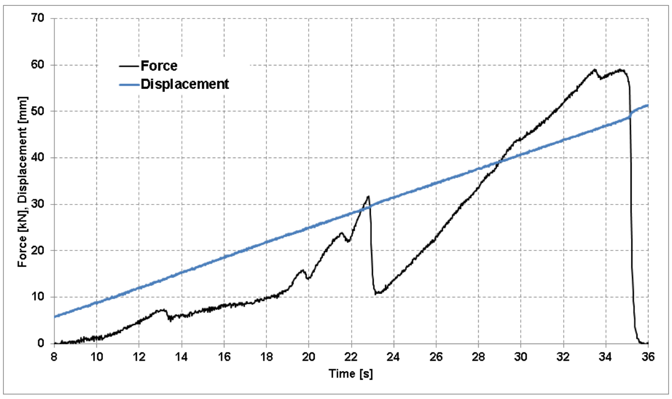

a) Loading of triangle ("narrow") specimen

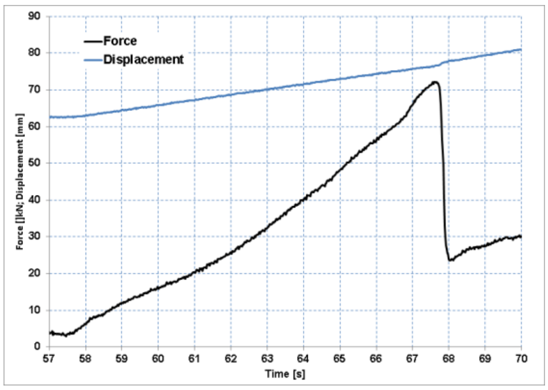

b) Loading of trapezium ("wide") specimen

Figure 8. Time records of force and plate displacement

a) formation of first crack due to bending

b) opening of the first crack

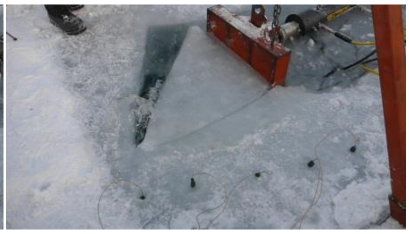

c) specimen is fully separated from ambient ice due to shear

Figure 9. Testing of triangle ("narrow") specimen

Figure 10. View of trapezium ("wide") specimen after testing.

Two phases of macro crack development were observed in the loading tests of the narrow (triangular) specimen:

– Indentation of vertical plate into ice causing ice crushing and load growth; initiation of a macro crack in the root section of the specimen caused by bending moment (peak load $F_1 = 32$ kN at instant $t_1 = 22.8$ s Figure 9a). A simple formula from the beam bending theory gives the ice bending strength in horizontal plane of $\sigma_f = 0.229$ MPa. This value practically coincides with the value $\sigma_f = 0.231$ MPa obtained by the authors from bending tests of cantilever ice beams in horizontal plane in the same ice. From Figures 9a and 9b it is seen that a bending crack does not propagate across the entire root section: its length is about 0.56 m, while the root section length is 0.7 m.

– Under further loading of the specimen the force is growing monotonously for almost 11 seconds (till $t_2 = 33.6$ s). At $F_2 = 60$ kN, corresponding to the second peak value, the specimen is fully splitted. Limit stresses at failure in this case can be estimated from: $\sigma_{lim} = \frac{F_2}{h \cdot a}$, where $h = 0.6$ m – ice thickness, $a = 0.14$ m –length of root section subject to failure. The obtained limit stress $\sigma_{lim} = 0.714$ MPa is in good agreement with other tests performed by the authors in the same ice using a similar loading setup with simulation of shearing failure. The average stress value in these tests was $\sigma_{lim} = 0.750$ MPa.

In loading test of the wide (trapezium) specimen the load monotonously increased as the plate penetrated the ice specimen. When the applied horizontal load reached 72 kN, a macro crack was initiated, which broke the specimen away from the ice field. In comparison with the failure (split) of the narrow specimen it should be note that in this case:

– The specimen was split in one step, i.e. the load gradually increased up to the limit value and then dropped practically at once after the macro crack was made.

– Unlike the triangular specimen, when the crack practically ran across the root section, the wide specimen had an L-shaped crack. It is an evidence of a complex stress state of the split ice section and a simplified analysis of the crack initiation and propagations will not work in this case.

Analytical stress/strain studies for ice cantilever specimens of triangular shape (wedges) under a horizontal force are described below.

LIMIT STRESS ANALYSIS OF ICE WEDGES UNDER HORIZONTAL LOADING

Let us consider a two-dimensional problem of an ice cantilever wedge-shaped specimen being loaded with a horizontal force uniformly distributed over one edge of the specimen, assuming that ice is a homogeneous material. A narrow wedge AOB (Figure 11a) will fail under the load when the stress in extreme tensioned fibers reaches the tensile ice strength limit. In this case ice stressed state is close to tension-compression and the bending theory provides a rather good approximation of the limit load p causing failure by propagation of a splitting crack AB. For larger angles $2\alpha > 45°$ (in case of a wide wedge base) a 2D stressed state can be analyzed using the limit curve shown in Figure 11b (Schulson and Duval, 2009).

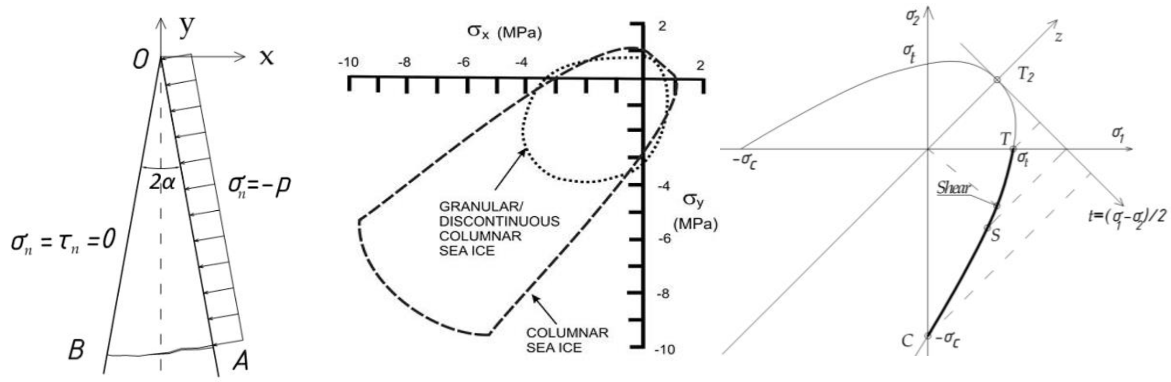

a) Narrow wedge loading with uniformly distributed over one edge pressure

b) Failure envelope of sea ice

c) Representation of limit curve segment as a parabola

Figure 11. Scheme of narrow wedge loading and ice strength diagrams

The stressed state of wedge-shaped ice specimen is located in the fourth quadrant of the principle stress plane. Let us represent the limit curve as a parabola (Figure 11c) passing through two points: C $(0; -\sigma_c)$ – ice compression strength and T $(\sigma_t; 0)$ – ice tensile strength. The parabola axis lies on the bisectrix of the first quadrant: $\sigma_1 = \sigma_2$. The parabolic equation in terms of new variables $t = (\sigma_1 - \sigma_2)/2$ and $z = (\sigma_1 + \sigma_2)/2 - \sigma_0$ is written as

$$f(\sigma_1, \sigma_2) = z + At^2 = 0 \qquad (1)$$

where $A = 2/(\sigma_c - \sigma_t)$. Other characteristic points of the parabola are as follows:

$T_2 = (\sigma_0, \sigma_0)$ – parabola apex corresponding to the strength under bi-axial tensioning $\sigma_0 = \dfrac{\sigma_c \sigma_t}{2(\sigma_c - \sigma_t)}$, and point $(\tau_s; -\tau_s)$, where $2\tau_s = \sqrt{\sigma_c \sigma_t}$ – uniaxial shear strength.

The statement of problem on limiting wedge equilibrium is reduced to equilibrium equations in the polar coordinate system

$$\begin{cases} \sigma_r - \sigma_\theta + \dfrac{d\tau_{r\theta}}{d\theta} = 0 \\ \dfrac{d\sigma_\theta}{d\theta} + 2\tau_{r\theta} = 0 \end{cases} \qquad (2)$$

where stress components are dependent only on the angle Θ and related by the principal stresses

$$\begin{cases} \sigma_r = \dfrac{\sigma_1 + \sigma_2}{2} + \dfrac{\sigma_1 - \sigma_2}{2}\cos 2\psi = z + \sigma_0 + t\cos 2\psi \\ \sigma_\theta = \dfrac{\sigma_1 + \sigma_2}{2} - \dfrac{\sigma_1 - \sigma_2}{2}\cos 2\psi = z + \sigma_0 - t\cos 2\psi \\ \tau_{r\theta} = \dfrac{\sigma_1 - \sigma_2}{2}\sin 2\psi = t\sin 2\psi \end{cases} \qquad (3)$$

Equation (2) at limit conditions (1) may have two solutions – discontinuous stress field and continuous one (Figure 12).

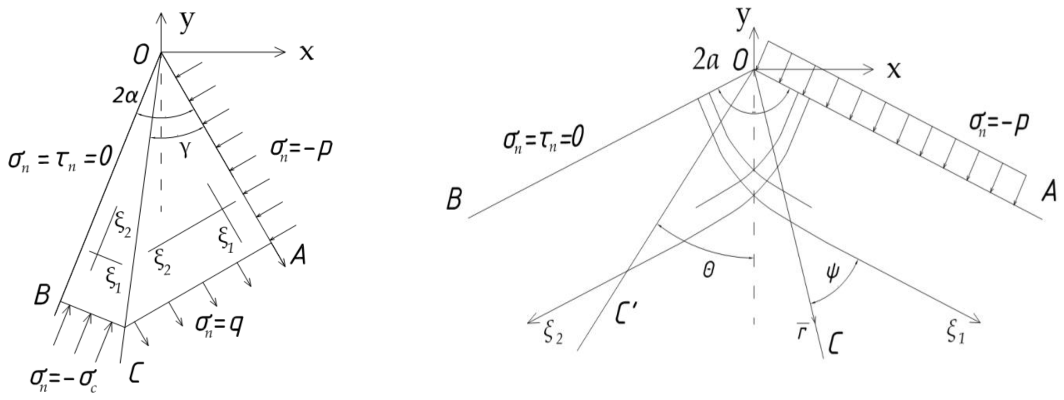

a) Discontinuous stress field   b) Continuous stress field

Figure 12. Two solutions for a wedge loading

Let us find the solution based on the discontinuous stress field for a wedge with angle 2α (Figure 12a). Considering that stresses on the boundary OB are equal to zero, the stressed state within the triangle OBC is uniform $(0; -\sigma_c)$. At the section OA stresses are equal to $\sigma_n = -p$, $\tau_n = 0$, the stressed state within the triangle OAC is also uniform $(q; -p)$, $q \le \sigma_t$, and corresponds to the parabola arc CT (Figure 11c). After reducing the stresses into non-dimensional form, dividing the same by σ_c and introducing $\mu = \sigma_t / \sigma_c < 1$, $s_1 = q/\sigma_c$; $s_2 = -p/\sigma_c$, we can re-write the parabolic equation as follows

$$(s_1 - s_2)^2 + (1-\mu)(s_1 + s_2) - \mu = 0 \qquad (4)$$

For matching the stress fields on the section OC let us write the equilibrium equation $[\sigma_n] = [\tau_n] = 0$. The equilibrium conditions and limit curve equation (4) are equivalent to the transcendental equation

$$\frac{\sin^2 2(2\alpha - \gamma)}{\sin^2 2\gamma} + 2\cdot(1-\mu)\frac{\sin(2\alpha - \gamma)\cos(2\alpha + \gamma)}{\sin 2\gamma} - \mu = 0 \qquad (5)$$

where γ – angle between the sections OA and OC. Eq. (5) can be solved either numerically or graphically.

If the ratio between tensile-to-compression ice strength is assumed $\mu = \sigma_t / \sigma_c = 0.25$, then from (5) for a wedge with angle $2\alpha = 45°$ we obtain $\gamma = 30.3°$. The limit load on OA in this case is $p = 0.84\sigma_t$, and tension on AC is $q = 1.04\sigma_t$, i.e. the stressed state in the triangle OAC is very close to the uniaxial shear, while the limit load on the wedge is just a little bit higher than the ice tensile strength.

The performed theoretical analysis examines the stressed state of ice wedge prior to initiation of the first crack. The theory is not extended to stage after first crack formation in the case when the ice wedge is broken in two (or more) steps as during the tests on the "narrow" specimen in sea ice (Figures 8a and 9).

CONCLUSIONS

Ice field splitting is quite a probable scenario of ice interaction with an engineering structure partly sheltered by another structure. The global ice load on the structure in this case is governed by the force required to break off a large ice floe being a cantilever beam of wedge or truncated wedge shape. The results obtained in model tests show that the maximum ice loads correspond to the values calculated from the simple beam bending theory. Two meso scale tests in sea ice with horizontal loading of short cantilever ice specimens indicate that the ice failure patterns depend on the specimen geometry. Based on the theoretical analysis of 2D stressed state of wedge-shaped ice specimens possible mechanisms of ice failure are identified: for relatively narrow specimens the breaking force may be estimated using the theory of cantilever beam bending, while the wide specimens may be subject to shear failure.

ACKNOWLEDGEMENTS

The authors wish to acknowledge the support of the Research Council of Norway through the Center for Sustainable Arctic Marine and Coastal Technology (SAMCoT).

REFERENCES

Berger, J., 2008. Ice protection structures. Journal Schiff&Hafen, No.6, pp.16-18.

Bhat, S.U., 1988. Analysis for splitting of ice floes during summer impact. In Cold Regions Science and Technology, 15, pp. 53-63.

International Standard ISO 19906, 2011. Petroleum and natural gas industries – Arctic offshore structures.

Karulina M., Karulin E., Blagovidova I., Bardin I., 2012. Experience of enhancing ice resistance of platforms for exploring North Caspian oil and gas fields. Transactions of KSRC, Issue 70 (354), St.Petersburg, pp.83-98.

Schulson, E.M., Duval, P., 2009. Creep and Fracture of Ice. Cambridge University Press.

Prager W. and Hodge Ph.G., 1951. Theory of perfectly plastic solids. N.Y.

Sodhi D.S. and Chin S.N., 1995. Indentation and splitting of freshwater ice floes. Journ. of Offshore Mechanics and Arctic Engineering. Vol. 117, pp. 63-69